

Nature of the first-order antiferromagnetic-ferromagnetic transition in the Ge-rich magnetocaloric compounds $Gd_5(Si_xGe_{1-x})_4$

L. Morellon, J. Blasco, P. A. Algarabel, and M. R. Ibarra*

Departamento de Física de la Materia Condensada and Instituto de Ciencia de Materiales de Aragón, Universidad de Zaragoza and Consejo Superior de Investigaciones Científicas, 50009 Zaragoza, Spain

(Received 14 January 2000; revised manuscript received 18 April 2000)

We report that the first-order antiferromagnetic to ferromagnetic transition in the Ge-rich magnetocaloric compound $Gd_5(Si_{0.1}Ge_{0.9})_4$ is associated with a structural phase transformation from a high-temperature Gd_5Ge_4 -type $Pnma$ to a low-temperature Gd_5Si_4 -type $Pnma$ orthorhombic structure. This magnetostructural transition can be triggered reversibly by application of an external magnetic field, resulting in strong magnetoelastic effects above the transition. The revised magnetic and crystallographic phase diagram for the $Gd_5(Si_xGe_{1-x})_4$ series is proposed.

I. INTRODUCTION

A giant magnetocaloric effect (MCE) has been recently discovered in the $Gd_5(Si_xGe_{1-x})_4$ pseudobinary system with $x \leq 0.5$,¹⁻³ making these alloys potential candidates for magnetic refrigeration in the range ~ 20 – ~ 290 K.⁴ The composition range $0.24 \leq x \leq 0.5$ is of special interest since the MCE is related to a first-order phase transition from a high-temperature paramagnetic to a low-temperature ferromagnetic state, at temperatures ranging from 130 K ($x = 0.24$) to 276 K ($x = 0.5$).² A recent study of the $Gd_5(Si_{0.45}Ge_{0.55})_4$ alloy has revealed that on cooling this transition is associated with a first-order structural transition from a monoclinic (paramagnetic, space group $P112_1/a$) to an orthorhombic (ferromagnetic, space group $Pnma$) symmetry.⁵ The following detailed crystal structure determination of both orthorhombic and monoclinic phases in a $Gd_5(Si_{0.5}Ge_{0.5})_4$ single crystal was carried out in Ref. 6. This magnetostructural transition can be induced reversibly by application of an external magnetic field, resulting in strong magnetoelastic effects⁵ and a giant negative magnetoresistance.^{7,8} Therefore these alloys are also attractive in view of their potential technological applications for magnetostrictive/magnetoresistive transducers.

The magnetic behavior of the Ge-rich compounds with $x \leq 0.2$ differs from the aforementioned and also from that found in the Si-rich ($x > 0.5$) region. The magnetic phase diagram and a comprehensive room-temperature structural characterization can be found in Ref. 9. Both Ge-rich and Si-rich alloys crystallize in the orthorhombic system (space group $Pnma$) and earlier¹⁰ were thought to have the same crystal structure. Nevertheless, the Si-based compounds are ferromagnets (second-order para-ferromagnetic transition), while the Ge alloys order antiferromagnetically (or ferrimagnetically) at $T_N \cong 125$ K (second-order paraantiferromagnetic transition), and then experience a further first-order transition to a low-temperature ferromagnetic state.² This transition ranges linearly from $T_C \cong 20$ K ($x = 0$) to $\cong 120$ K ($x = 0.2$). Interestingly, a giant MCE has also been observed at this transition,² despite its entirely different magnetic origin. Although recent direct measurements

of the adiabatic temperature change in $Gd_5(Si_{0.5}Ge_{0.5})_4$ show a smaller magnetocaloric effect,¹¹ the $Gd_5(Si_xGe_{1-x})_4$ system offers a rather unique scenario where a close relation between crystallographic and magnetic degrees of freedom leads to the rich phenomenology described. Therefore further experimental and theoretical studies may be of great significance and future impact.

The aim of this contribution is to gain new understanding on the nature of the first-order antiferromagnetic-ferromagnetic transition in the Ge-rich magnetocaloric compounds $Gd_5(Si_xGe_{1-x})_4$. We report a magnetic and crystallographic experimental study of the $Gd_5(Si_{0.1}Ge_{0.9})_4$ alloy, demonstrating that the transition in question occurs simultaneously with a crystallographic transformation between two $Pnma$ orthorhombic structures (high-temperature Gd_5Ge_4 type to a low-temperature Gd_5Si_4 type). A comparison with the crystallographic and magnetic behavior of the rest of the series will be made, and a revised magnetic and crystallographic temperature-composition phase diagram for the $Gd_5(Si_xGe_{1-x})_4$ magnetocaloric materials is proposed.

II. EXPERIMENT

The alloy with nominal composition $Gd_5(Si_{0.1}Ge_{0.9})_4$ was synthesized by arc melting of 99.9 wt% pure Gd and 99.9999 wt% pure Si and Ge (all elements purchased from Alfa Aesar®) under a high-purity argon atmosphere. Weight losses during melting were negligible and therefore the initial composition was assumed unchanged. The quality of the sample was checked by x-ray diffraction and scanning electron microscopy. The room-temperature x-ray pattern confirms the presence of an orthorhombic main phase ($Pnma$) with the unit-cell parameters $a = 7.6887(1)$ Å, $b = 14.827(2)$ Å, and $c = 7.7785(1)$ Å, in good agreement with those reported in Ref. 9 for similar compositions. A minor amount of a secondary phase has also been detected and indexed as hexagonal $Gd_5(Si, Ge)_3$. This secondary phase was also seen by scanning electron microscopy but the observed regions were too narrow (≤ 2 μm) for a quantitative composition determination by electron-beam microprobe analysis. The ac magnetic susceptibility was measured using

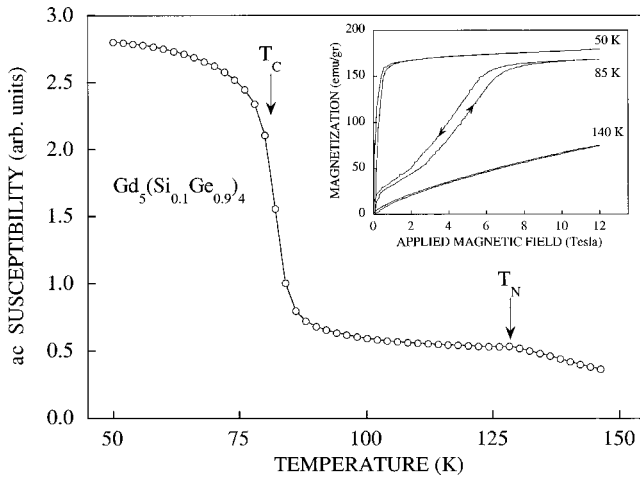


FIG. 1. ac magnetic susceptibility (χ_{ac}) of $\text{Gd}_5(\text{Si}_{0.1}\text{Ge}_{0.9})_4$ as a function of temperature. The different magnetic phase transition temperatures are indicated: On heating, the system undergoes a first-order ferromagnetic-to-antiferromagnetic transition at T_C and a subsequent second-order transition to the paramagnetic state at T_N . The inset shows magnetization isotherms up to 12 T at selected temperatures.

a commercial (Quantum Design) superconducting quantum interference device (SQUID) magnetometer with an excitation field of 1 Oe (peak value) at a frequency of 10 Hz. Magnetization isotherms were measured in a vibrating-sample magnetometer (VSM) (Oxford Instruments) up to 12 T. Step-scanned (step size = 0.02°) powder x-ray-diffraction patterns were collected at selected temperatures ranging from 30 to 300 K using a D-max Rigaku system with rotating anode using $\text{Cu } K\alpha_{1,2}$ radiation coupled to a helium flow cryostat between 20° and 80° (2θ). The pattern profiles were analyzed using the Rietveld refinement program FULLPROF (Ref. 12) with the lattice and atomic parameters determined at room temperature in Ref. 9 as starting values. Linear thermal-expansion and magnetostriction measurements were performed using the strain-gauge technique in a superconducting coil that produces steady magnetic fields of up to 12 T.

III. RESULTS AND DISCUSSION

The ac magnetic susceptibility of the $\text{Gd}_5(\text{Si}_{0.1}\text{Ge}_{0.9})_4$ sample in the temperature range 50–150 K is displayed in Fig. 1. The measurement was performed increasing the temperature after the sample had been zero-field cooled down to 5 K. An abrupt transition is clearly observed at $T_C = 81$ K (value taken at the maximum slope) in good agreement with the expected first-order magnetic transition from a low-temperature ferromagnetic (FM) ground state to an antiferromagnetic (AFM) phase.² The latter transforms into the paramagnetic state (PM) at a second-order transition at $T_N = 127$ K, seen as a small anomaly in the ac susceptibility. The behavior of the ac susceptibility as a function of temperature follows quite closely that reported in Ref. 13 for a similar composition ($x = 0.08$). To illustrate the different magnetic character of each phase, we have included as an inset in Fig. 1 magnetization isotherms in each relevant temperature range, i.e., ferromagnetic ($T = 50 \text{ K} < T_C$), antiferro-

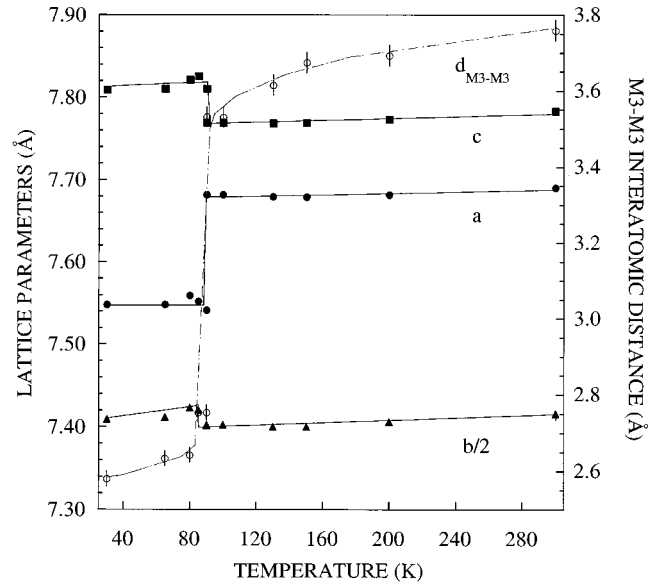


FIG. 2. Thermal dependence of the lattice parameters (closed symbols) and $M3-M3$, $M3 = 0.1 \text{ Si} + 0.9 \text{ Ge}$ at site $8d$, interatomic distance (open symbol) of $\text{Gd}_5(\text{Si}_{0.1}\text{Ge}_{0.9})_4$ as obtained from the Rietveld analysis of the x-ray powder-diffraction patterns. The orthorhombic space group $Pnma$ remains unchanged through the magnetostructural transition. The lines are a guide to the eye.

magnetic ($T_C < T = 85 \text{ K} < T_N$), and paramagnetic ($T = 140 \text{ K} > T_N$). In the antiferromagnetic phase, the ferromagnetic state can be reached by application of an external magnetic field through a first-order field-induced metamagnetic transition. Also, as can be observed at $T = 85 \text{ K}$, there is a rapid increase in the magnetization at low fields, suggesting the presence of a ferromagnetic component. This has not been observed in $x = 0.08$,¹³ and a contribution from the $\text{Gd}_5(\text{Si}, \text{Ge})_3$ impurity phase is unlikely since this orders at lower temperatures.¹⁴ A possible explanation could be the existence of an additional field-induced process along some specific direction, which would suggest that the antiferromagnetic phase is a complex canted ferrimagnetic structure, as pointed out in Ref. 13 and as observed in Nd_5Ge_4 (Ref. 15) and Tb_5Ge_4 .¹⁶ Further experimental studies are needed to confirm this point. The metamagnetic transition to the ferromagnetic state shifts with field to higher temperatures at a rate of $\approx 3.7 \text{ K/T}$. This value is in agreement to that obtained in $x = 0.08$,¹³ $\approx 3.4 \text{ K/T}$, and is also quite similar to that observed in the $0.24 \leq x \leq 0.5$ alloys [e.g., 4.3 K/T in $x = 0.43$,² 4.5 K/T in $x = 0.45$,⁵ and 5.5 K/T in $x = 0.5$ (Ref. 1)] despite its different magnetic origin, i.e., AFM-FM in $x \leq 0.2$ versus PM-FM in the $0.24 \leq x \leq 0.5$ range. This motivated a more detailed structural study by x-ray powder diffraction in the 30–300 K temperature range to probe the possible existence of associated structural effects at T_C .

Figure 2 shows the temperature dependence of the lattice parameters of $\text{Gd}_5(\text{Si}_{0.1}\text{Ge}_{0.9})_4$. In the whole temperature range, the x-ray patterns were refined in the same $Pnma$ orthorhombic space group. No significant change in the unit-cell parameters was observed at T_N . In contrast, abrupt changes are clearly seen when cooling through T_C : $\Delta a/a \approx -1.6\%$, $\Delta b/b \approx +0.3\%$, and $\Delta c/c \approx +0.7\%$. There is a remarkable resemblance with the structural transition in the

TABLE I. Space group, lattice parameters, unit-cell volume, fractional atomic coordinates, average thermal factor, and reliability factors (as defined in Ref. 12) of $\text{Gd}_5(\text{Si}_{0.1}\text{Ge}_{0.9})_4$ at 30 K (Gd_5Si_4 type) and 100 K (Gd_5Ge_4 type). Numbers in parentheses indicate standard deviation of the last digit. $M = 0.1 \text{ Si} + 0.9 \text{ Ge}$.

	30 K	100 K
Space group	<i>Pnma</i>	<i>Pnma</i>
<i>a</i> (Å)	7.548(1)	7.682(1)
<i>b</i> (Å)	14.818(2)	14.804(2)
<i>c</i> (Å)	7.809(1)	7.769(1)
<i>V</i> (Å ³)	873.4(3)	883.7(3)
Gd 1: <i>x</i>	0.348(2)	0.293(2)
<i>y</i>	$\frac{1}{4}$	$\frac{1}{4}$
<i>z</i>	0.002(1)	-0.008(2)
Gd 2: <i>x</i>	0.015(1)	-0.024(1)
<i>y</i>	0.099(1)	0.097(1)
<i>z</i>	0.193(1)	0.172(1)
Gd 3: <i>x</i>	0.325(1)	0.379(1)
<i>y</i>	0.876(1)	0.878(1)
<i>z</i>	0.179(1)	0.169(1)
M1: <i>x</i>	0.204(2)	0.171(3)
<i>y</i>	$\frac{1}{4}$	$\frac{1}{4}$
<i>z</i>	0.370(2)	0.371(3)
M2: <i>x</i>	0.956(3)	0.920(3)
<i>y</i>	$\frac{1}{4}$	$\frac{1}{4}$
<i>z</i>	0.901(2)	0.887(3)
M3: <i>x</i>	0.141(2)	0.213(2)
<i>y</i>	0.951(1)	0.957(1)
<i>z</i>	0.486(2)	0.480(2)
B_{av} (Å ²)	0.12(11)	0.14(12)
R_p/R_{wp} (%)	6.2/7.9	6.6/8.3
R_{Bragg} (%)	6.1	6.5
χ^2	1.2	1.3

$x=0.45$ (Ref. 5) and the $x=0.5$ alloys,⁶ i.e., when cooling the sample the main lattice change is also seen as a drastic reduction in the *a* axis, that cannot be fortuitous. Nevertheless, we must point out that, unlike the $x=0.45$ and $x=0.5$ alloys, *here the symmetry remains unchanged through the transition*. A similar unit-cell behavior also occurs at room temperature upon the change in chemical composition from the Si- to the Ge-rich compounds.⁹ The Rietveld-refined lattice parameters and fractional atomic coordinates at two selected temperatures, $T=30 \text{ K} < T_C$ and $T_C < T=100 \text{ K} < T_N$, are listed in Table I. The comparison of the observed and calculated x-ray-diffraction patterns at both temperatures is shown in Fig. 3. Our results indicate that the low-temperature crystallographic phase is quite similar to the Gd_5Si_4 -type one reported for the Si-rich ($x > 0.5$) alloys.⁹ Furthermore, according to Pecharsky and Gschneidner,⁹ the largest change in the interatomic distances in Gd_5Ge_4 -based compounds compared to the Gd_5Si_4 -based ones at room temperature occurs in the vicinity of the M3 atom at the $8d$ site, $M = x\text{Si} + (1-x)\text{Ge}$. In the Gd_5Ge_4 -based compounds, the M3 atom loses the other M3 as nearest neighbors, which is exactly what is seen in $\text{Gd}_5(\text{Si}_{0.1}\text{Ge}_{0.9})_4$ when heating through T_C . This has been illustrated in Fig. 2 by plotting the M3-M3 interatomic distance as a function of temperature. A

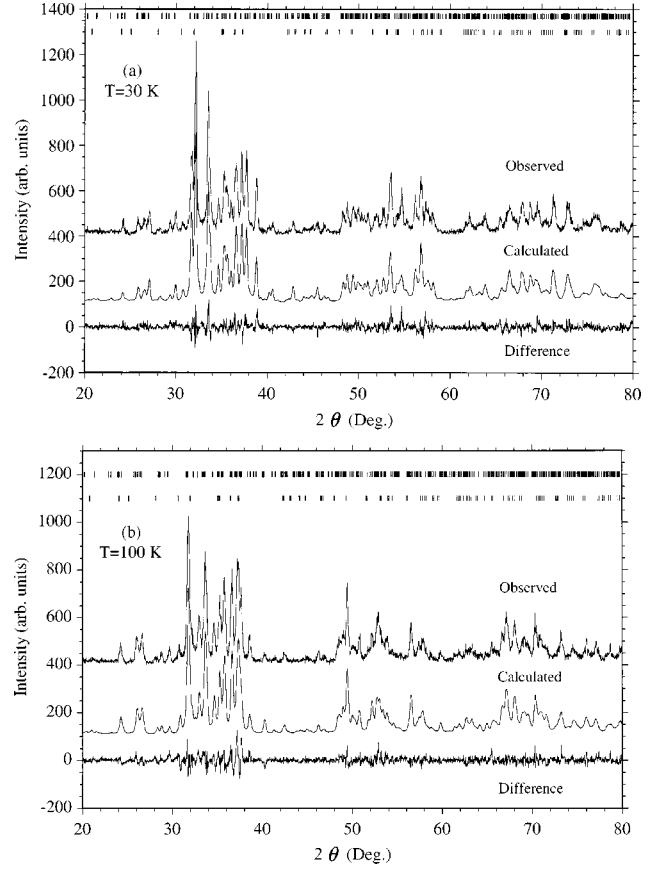


FIG. 3. X-ray powder-diffraction patterns of $\text{Gd}_5(\text{Si}_{0.1}\text{Ge}_{0.9})_4$ at 30 K (a) and 100 K (b). Both observed and calculated patterns are included for comparison, and their difference. The allowed Bragg reflections for the main 5:4 phase and the secondary hexagonal 5:3 phase are indicated at the top of the figures.

huge increase of $\cong 34\%$ is observed, reflecting indeed the changes in the atomic environment. Preferred orientation along the [100] direction has been detected and accounted during the refinements. We have obtained a textured fraction of the sample of 20% at 100 K and 12% at 30 K. In the experiment, the powder was mixed with a low-temperature paste (Apiezon-T) to minimize the texture effects and ensure a good thermal contact. Nevertheless, a compromise with the rather large background observed in the diffraction profiles due to the amorphous contribution from this paste had to be reached. We have confirmed that this texture introduces errors in the refined atomic coordinates and thermal displacement factors (the Si/Ge distribution in each of the three *M* sites has been constrained to the nominal 10% Si and 90% Ge). In consequence, our results, although qualitatively correct, should be regarded as preliminary. A detailed crystal structure determination by single-crystal x-ray diffraction is thus strongly required. At 90 K, coexistence of both crystallographic phases is observed, in agreement with the first-order character of the transition. Our results demonstrate that the observed first-order AFM-FM phase transition in the Ge-rich ($x \leq 0.2$) $\text{Gd}_5(\text{Si}_x\text{Ge}_{1-x})_4$ materials takes place simultaneously with a structural transformation from a high-temperature orthorhombic Gd_5Ge_4 -type *Pnma* structure to a low-temperature orthorhombic Gd_5Si_4 -type *Pnma* one.

An important question would be whether this magneto-

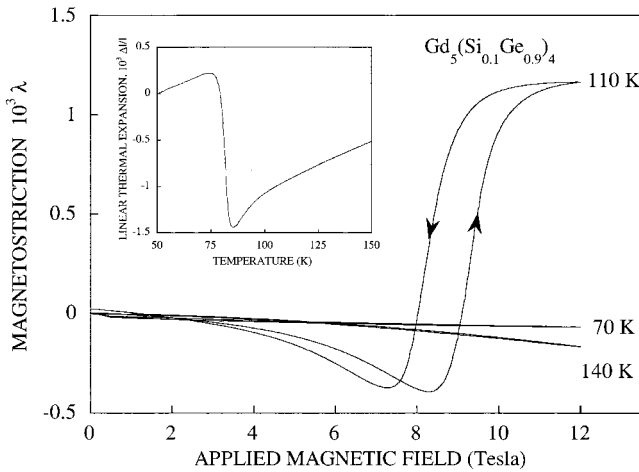


FIG. 4. Magnetostriction isotherms (λ) along the applied field at selected temperatures. The inset shows the linear thermal expansion ($\Delta l/l$) as a function of (increasing) temperature along the same measurement direction.

structural transition can be induced reversibly by the application of an external magnetic field. Magnetostriction isotherms at selected temperatures ($T = 70 \text{ K} < T_C$, $T_C < T = 110 \text{ K} < T_N$, $T = 140 \text{ K} > T_N$) along the applied magnetic field are shown in Fig. 4 together with the linear thermal expansion in the 50–150 K temperature range (inset) measured along the same direction. No significant magnetoelastic effects are observed except in the AFM region. It can be seen that at a certain critical field the lattice expands by the same amount as the observed spontaneously ($H=0$) as a function of temperature at T_C , $\Delta l/l \cong 0.16\%$ (see the inset). It should be noted that this change in the lattice, when compared with the x-ray results (see Fig. 2), reflects a strong texture, probably in a plane containing predominantly b and c axes, of the fragment of the sample used for these measurements. This texture is inherent in the sample preparation method used and, although minimized, has also been detected during the x-ray-diffraction refinements as explained previously.

From the thermal dependence of the critical field, we can estimate an averaged value (increasing and decreasing field) of $dT_C/dH \cong 3.7(1) \text{ K T}$ in very good agreement from that obtained from magnetization. Consequently, these results indeed demonstrate, that the observed magnetostructural transition at T_C can be induced reversibly by an applied magnetic field, which is in agreement with the specific heat data for $x=0.08$ in Ref. 13. In addition, we may predict that if a single crystal of this composition were grown and measured along the a axis, a giant magnetoelastic effect as large as $\Delta l/l \cong 1.6\%$ could be achieved by application of a magnetic field in the AFM phase. This would be one of the largest reported reversible magnetoelastic effect, only comparable with that found in, e.g., MnAs ,¹⁷ TbMn_2 ,¹⁸ and quite recently in Ni_2MnGa (6.1% at room temperature).¹⁹ Similar values also associated with a change in the crystal structure have been reported in a DyCu_2 single crystal,²⁰ although in this case the effect is irreversible.

Based on the experimental results presented so far, we can propose a revised magnetic and crystallographic temperature-composition phase diagram for the

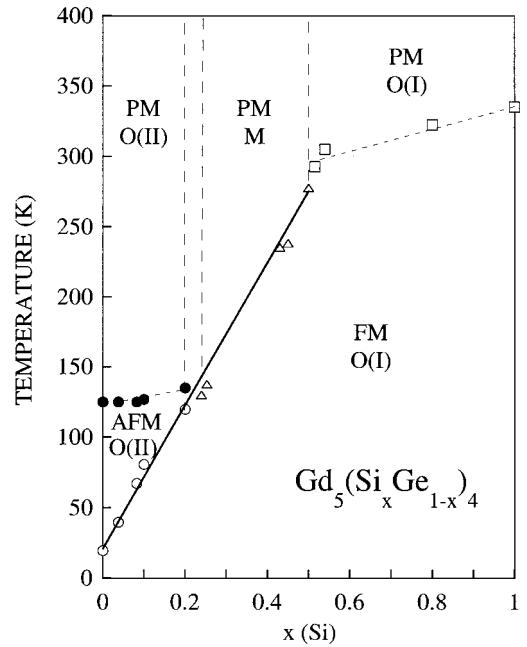


FIG. 5. Magnetic and crystallographic temperature-composition phase diagram of the $\text{Gd}_5(\text{Si}_x\text{Ge}_{1-x})_4$ materials. PM, FM, and AFM label different magnetic phases and $O(I)$, M , and $O(II)$ denote different crystallographic structures, as defined throughout the text. The transition temperatures have been taken from Refs. 2 and 9; $x=0.45$ from Ref. 5, and $x=0.1$ from the present work. The solid line indicates a first-order magnetostructural phase boundary.

$\text{Gd}_5(\text{Si}_x\text{Ge}_{1-x})_4$ materials, see Fig. 5. The different magnetic transition temperatures have been taken from Refs. 2 and 9, together with our data for $x=0.45$,⁵ and $x=0.1$. The different magnetic phases have been indicated as before: PM (paramagnetic), FM (ferromagnetic), and AFM (antiferromagnetic/ferrimagnetic). Following the notation used in Ref. 9, $O(I)$, M , and $O(II)$ stand for the different crystallographic phases: $O(I)$ is a Gd_5Si_4 -type $Pnma$ orthorhombic structure, M denotes $P1121/a$ monoclinic, and $O(II)$ the Gd_5Ge_4 -type $Pnma$ orthorhombic structure. In the $0.24 \leq x \leq 0.5$ region, the magnetostructural transition is an $O(I) \leftrightarrow M$ transformation.⁶ It is noteworthy that the ground state for all the $\text{Gd}_5(\text{Si}_x\text{Ge}_{1-x})_4$ compounds is the Gd_5Si_4 -type orthorhombic $Pnma$ ferromagnetic phase [FM- $O(I)$]. Therefore we can conclude that despite the different magnetic origin of the observed transitions, a giant MCE and magnetostriction (and most likely giant magnetoresistance as reported for some room-temperature monoclinic compositions)^{7,8} are obtained when crossing the low-temperature first-order phase boundary toward the ground state, indicated as a thick solid line in Fig. 5. Regarding the correlation between crystallographic and magnetic phases, it has been proposed that the presence or absence of covalently bonded Si(Ge)-Si(Ge) pairs has the most important impact on the Ruderman-Kittel-Kasuya-Yosida interaction between the Gd ions.⁶ More specifically, these authors have suggested that the number of covalent bonds decreases from the $O(I)$ to the M , and from the M to the $O(II)$ phase, thus decreasing the number of the conduction electrons available. This, in addition to the corresponding decrease in the cell volume, leads to a strong increase in the Fermi wave vector, therefore explaining the change in sign of the exchange interaction in the

O(II) phase. Although this simple picture is quite satisfactory, it might be argued that other effects could be of importance. For instance, the role of the Gd *5d* electrons in the indirect exchange interaction, as suggested by Szade and Skorek.²¹ Another model²² emphasizes that the density of states at the Fermi level is the relevant factor determining the sign of the conduction-band indirect exchange interaction. In order to establish quantitatively the effect of these possible contributions and gain a deeper understanding of the relationship between crystallography and magnetism in these compounds, further theoretical band-structure calculations and theoretical work are urgently needed.

In summary, we have found that the first-order antiferromagnetic-to-ferromagnetic transition in the Ge-rich magnetocaloric compounds $\text{Gd}_5(\text{Si}_x\text{Ge}_{1-x})_4$ ($x \leq 0.2$) is as-

sociated with a structural transformation from a high-temperature Gd_5Ge_4 -type Pnma to a low-temperature Gd_5Si_4 -type Pnma orthorhombic structure. The revised magnetic and crystallographic phase diagram of the $\text{Gd}_5(\text{Si}_x\text{Ge}_{1-x})_4$ alloys is proposed. The FM-*O*(I) phase is the ground state in the whole composition range, and important magnetoelastic effects are observed when crossing the low-temperature first-order phase boundary toward this ground state.

ACKNOWLEDGMENT

The financial support of the Spanish CICYT under Grant No. MAT99-1063-C04 is acknowledged.

*Corresponding author: Prof. M. R. Ibarra, Departamento de Física de la Materia Condensada, Facultad de Ciencias, Universidad de Zaragoza, Pedro Cerbuna 12, 50009 Zaragoza, Spain. Email address: ibarra@posta.unizar.es FAX: 34-976-761229.

¹V. K. Pecharsky and K. A. Gschneidner, Jr., *Phys. Rev. Lett.* **78**, 4494 (1997).

²V. K. Pecharsky and K. A. Gschneidner, Jr., *Appl. Phys. Lett.* **70**, 3299 (1997).

³V. K. Pecharsky and K. A. Gschneidner, Jr., *J. Magn. Magn. Mater.* **167**, L179 (1997).

⁴V. K. Pecharsky and K. A. Gschneidner, Jr., *J. Magn. Magn. Mater.* **200**, 44 (1999).

⁵L. Morellon, P. A. Algarabel, M. R. Ibarra, J. Blasco, B. García-Landa, Z. Arnold, and F. Albertini, *Phys. Rev. B* **58**, R14 721 (1998).

⁶W. Choe, V. K. Pecharsky, A. O. Pecharsky, K. A. Gschneidner, Jr., V. G. Young, Jr., and G. J. Miller, *Phys. Rev. Lett.* **84**, 4617 (2000).

⁷L. Morellon, J. Stankiewicz, B. García-Landa, P. A. Algarabel, and M. R. Ibarra, *Appl. Phys. Lett.* **73**, 3462 (1998).

⁸E. M. Levin, V. K. Pecharsky, and K. A. Gschneidner, Jr., *Phys. Rev. B* **60**, 7993 (1999); E. M. Levin, V. K. Pecharsky, K. A. Gschneidner, Jr., and P. Tomlinson, *J. Magn. Magn. Mater.* **210**, 181 (2000).

⁹V. K. Pecharsky and K. A. Gschneidner, Jr., *J. Alloys Compd.* **260**, 98 (1997).

¹⁰G. S. Smith, A. G. Tharp, and Q. Johnson, *Acta Crystallogr.* **22**, 940 (1967); F. Holtzberg, R. J. Gambino, and T. R. McGuire, *J.*

Phys. Chem. Solids **28**, 2283 (1967).

¹¹A. Giguère, M. Foldeaki, B. Ravi Gopal, R. Chahine, T. K. Bose, A. Frydman, and J. A. Barclay, *Phys. Rev. Lett.* **83**, 2262 (1999).

¹²J. L. Rodríguez-Carvajal, *Physica B* **55**, 192 (1992); J. L. Rodríguez-Carvajal and T. Roisnel, <http://www-llb.cea.fr/fullweb/fullprof.98/fp98.htm>

¹³V. K. Pecharsky and K. A. Gschneidner, Jr., *Adv. Cryog. Eng.* **43**, 1729 (1998).

¹⁴K. H. J. Buschow and J. F. Fast, *Phys. Status Solidi* **21**, 593 (1967); E. V. Ganapathy, K. Kugimiya, H. Steinink, and D. I. Tchernev, *J. Less-Common Met.* **44**, 245 (1976).

¹⁵P. Schobinger-Papamantellos and A. Niggli, *J. Phys. Chem. Solids* **42**, 583 (1981).

¹⁶P. Schobinger-Papamantellos, *J. Phys. Chem. Solids* **39**, 197 (1978).

¹⁷A. Zieba, Y. Shapira, and S. Foner, *Phys. Lett.* **91A**, 243 (1982).

¹⁸M. R. Ibarra, C. Marquina, L. García-Orza, and A. del Moral, *Solid State Commun.* **87**, 695 (1993).

¹⁹S. J. Murray, M. A. Marioni, A. K. Kukla, J. Robinson, R. C. O'Handley, and S. M. Allen, *J. Appl. Phys.* **87**, 5774 (2000).

²⁰P. Svoboda, M. Doerr, M. Loewenhaupt, M. Rotter, T. Reif, F. Bourdarot, and P. Burlet, *Europhys. Lett.* **48**, 410 (1999).

²¹J. Szade and G. Skorek, *J. Magn. Magn. Mater.* **196-197**, 699 (1999).

²²A. Hernando, J. M. Rojo, J. C. Gómez Sal, and J. M. Novo, *J. Appl. Phys.* **79**, 4815 (1996); A. Hernando, J. M. Barandiarán, J. M. Rojo, and J. C. Gómez Sal, *J. Magn. Magn. Mater.* **174**, 181 (1997).